J Membrane Biol (2008) 221:73–85
DOI 10.1007/s00232-007-9087-z

Predictions of the EC_{50} for Action Potential Block for Aliphatic Solutes

R. Hahin · J. Larsen · K. Gasser

Received: 3 July 2007 / Accepted: 12 November 2007 / Published online: 16 January 2008

Abstract Experiments were conducted to test the hypothesis that aliphatic hydrocarbons bind to pockets/crevices of sodium (Na^+) channels to cause action potential (AP) block. Aliphatic solutes exhibiting successively greater octanol/water partitition coefficients (K_{ow}) were studied. Each solute blocked Na^+ channels. The 50% effective concentration (EC_{50}) to block APs could be mathematically predicted as a function of the solute's properties. The solutes studied were methyl ethyl ketone (MEK), cyclohexanone, dichloromethane, chloroform and triethylamine (TriEA); the K_{ow} increased from MEK to TriEA. APs were recorded from frog nerves, and test solutes were added to Ringer's solution bathing the nerve. When combined with EC_{50}s for solutes with log K_{ow}s $<$ 0.29 obtained previously, the solute EC_{50}s could be predicted as a function of the fractional molar volume (dV/dm = [dV/dn]/100), polarity (P) and the hydrogen bond acceptor basicity (β) by the following equation: $EC_{50} = 2.612\left(10^{\{-2.117[dv/dm]+0.6424P+2.628\beta\}}\right)$ Fluidity changes cannot explain the EC_{50}s. Each of the solutes blocks Na^+ channels with little or no change in kinetics. Na^+ channel block explains much of the EC_{50} data. EC_{50}s are produced by a combination of effects including ion channel block, fluidity changes and osmotically induced structural changes. As the solute log K_{ow} increases to values near 1 or greater, Na^+ channel block dominates in determining the EC_{50}. The results are consistent with the hypothesis that the solutes bind to channel crevices to cause Na^+ channel and AP block.

Keywords Aliphatic solute · Sodium channel · Action potential · Effective blocking concentration · Membrane fluidity

R. Hahin (✉) · J. Larsen · K. Gasser
Biological Sciences Department, Northern Illinois University, DeKalb, IL 60115, USA
e-mail: hahin@niu.edu

Present Address:
J. Larsen
Global Pharmaceutical Research & Development, Abbott Laboratories, 100 Abbott Park Road, Department R4QF, AP9A-LL, Abbott Park, IL 60064-6115, USA

Introduction

The mechanism of general anesthesia is incompletely understood. General anesthesia is produced by a variety of substances possessing great structural diversity. Another group of diverse solutes can act as anesthetic or anesthetic-like agents and exhibit toxicity to humans and other vertebrates. However, local anesthetics comprise a less diverse group of substances and are known to block sodium channels (Strichartz et al., 1990) by binding to a distinct site on the channel protein. Possible explanations have been advanced to describe anesthesia include membrane fluidity changes (Mastrangelo et al., 1979) and the alteration of membrane proteins including ion channels caused by nonspecific anesthetic binding (Franks & Lieb, 1984). The potencies of anesthetics correlate well with their lipid solubility, as measured by their octanol water partition coefficient (K_{ow}). Since K_{ow} can be reliably predicted (Kamlet et al., 1981) as a function of several molecular properties (molar volume, hydrogen bonding acceptor basicity, polarity), it is instructive to examine the relationship between the chemical properties of a given compound and the production of action potential (AP) and Na^+ channel block.

In a previous study (Larsen, Gasser & Hahin, 1996), we employed voltage-clamp techniques to show that a group

of five solutes displaying a range of log K_{ow}s (from -1.35 to 0.1; log K_{ow}s < 0.29) acted to decrease the amplitude of Na^+ currents to cause AP block. In this current study, a group of five additional aliphatic and polychloroaliphatic solutes showing log K_{ow}s from 0.29 to 1.94 was chosen for study since they possess diverse properties, simple structures and K_{ow}s that have been well characterized (Taft et al., 1985). When the five solutes that display log K_{ow}s ≥ 0.29 (methyl ethyl ketone [MEK], cyclohexanone, dichloromethane [CH_2Cl_2], chloroform [$CHCl_3$] and triethylamine [TriEA]) are combined with the previously studied set of five solutes showing log K_{ow}s < 0.29 (dimethyl sulfoxide [DMSO], dimethyl formamide [DMF], *N,N*-dimethylacetamide [DMA], acetone, hexamethylphosphoramide [HMPA], they form an ordered set of 10 solutes with K_{ow}s that progressively decrease in value so that the set shows a >1,900-fold decrease in their values from 87 to 0.045. Included in this set of solutes is chloroform, which was first used as an anesthetic in 1847 and last used clinically in the United States in 1960. Its use was discontinued because of its toxicity to the liver and kidneys.

In this study, we obtained a concentration-response relation for solute-induced block of propagated APs in desheathed sciatic nerves for each solute. The concentrations blocking 50% of the AP height (EC_{50}) were then derived from each concentration-response relation. When the EC_{50}s of the solutes that exhibit log K_{ow}s ≥ 0.29 are combined with the EC_{50}s of the solutes that display log K_{ow}s < 0.29 (Larsen et al., 1996), they form a set that varies with, and can be mathematically predicted as a function of, the fractional molar volume (dV/dm), polarity (P) and hydrogen bond acceptor basicity (β) of the solutes.

In order to assay for solute-induced fluidity changes, we examined the ability of each of the solutes to alter membrane fluidity-sensitive chloride channel transport in secretory granule membranes. These experiments suggest that decreases in AP height appear at concentrations well below levels that produce fluidity changes.

Similar to the solutes previously studied (Larsen et al., 1996), the current set of solutes, displaying log K_{ow}s ≥ 0.29, also act to block Na^+ currents with little change in their kinetic properties; however, they are much more potent and block Na^+ currents and APs at much lower concentrations. In total, the experiments suggest that AP nerve block by all 10 aliphatic solutes is predominantly caused by sodium channel block. Solute size (dV/dm), polarity and hydrogen bond acceptor ability are important chemical properties that predict solute potency in producing AP block. The results are consistent with the hypothesis that a chemically diverse group of molecules bind to appropriately sized crevices on the surface of Na^+ channels and act to block Na^+ currents to cause AP block. In addition, molecules that display log K_{ow}s ≥ 0.29 have better access to the complete set of crevices and act as more potent "anesthetic-like" molecules.

Methods

Single Sucrose-Gap Technique

Solutes to be tested were dissolved in Ringer's solution and applied to isolated frog (*Rana pipiens*) sciatic nerves. Compound APs were elicited and recorded using a technique adapted from Hahin & Strichartz (1981) and briefly described below. A sciatic nerve was placed in a chamber so that the nerve spanned three compartments. The proximal end (placed in the intracellular compartment) was bathed in isosmotic KCl, and the middle (placed in the extracellular compartment) was bathed in either control Ringer's solution or a test solution and separated from KCl by a partition through which 0.22 M sucrose flowed. Sucrose flow was maintained constant (ca. 3–8 ml/min) throughout the recording period. The distal end of the nerve was bathed in Ringer's solution, which was covered by a layer of paraffin oil. APs were elicited by supramaximally stimulating the distal end of the nerve at a fixed rate (typically 1 pulse/10 min). Stimuli were delivered to the nerve by the use of chlorided silver wires and a model SD9 stimulator (Grass Instrument, Quincy MA). A brief (100 μs) supramaximal voltage pulse was used to elicit APs (typically 300–800 m*V*). APs were differentially recorded using Ag/AgCl electrodes by obtaining the potential in the intracellular compartment relative to the potential in the extracellular compartment; the extracellular pool was grounded via a third Ag/AgCl electrode. APs were recorded on photographs using a CR10 camera (Polaroid, Cambridge, MA) from repetitively applied traces on a 502A oscilloscope with 1 MHz bandwidth (Tektronix, Beaverton, OR). No filtering or preamplification was used.

Ringer's solution was applied to nerves to establish a control AP height and shape before applying any test solutes to the nerve. After applying solutes in Ringer's solution to whole nerves and recording APs, the solution bathing the nerve was removed and replaced with Ringer's solution. In order to ensure complete removal of the solutes, at minimum, three volume replacements (washouts) of the extracellular pool were made. Typically, the responses of five to nine nerves were measured for each solute tested.

Voltage-Clamp Technique

Single muscle fibers were dissected from the semitendinosus muscle of grass frogs (*R. pipiens*) and studied using

the Vaseline-gap voltage-clamp technique (Hille & Campbell, 1976). Changes in the original method were used in the experiments (Hahin & Campbell, 1983; Hahin, 1988). These changes produced a decrease in series resistance (0.5–1.5 Ω cm^2) and electrically uncoupled surface membrane currents from transverse-tubular currents so that surface Na^+ currents could be recorded in virtual isolation. The technique is more fully described in Larsen et al. (1996).

Voltage-clamp command pulses were generated by a digital stimulator (fabricated by R. H.). The stimulator timing was controlled by a Digitimer D4030 (Medical Systems, Great Neck, NY). Linear leakage and capacity current subtraction from original records was performed using an analogue electronic transient generator (constructed by R. H.). The subtracted records were filtered using a 40-kHz Bessel filter. Current records were sampled every 10 μs for a 12-ms duration using a Nicolet (Madison WI) 2090 digital storage oscilloscope and stored for later analysis. The sampling duration permitted the recording of currents prior to, during and after the application of a command pulse.

In order to isolate Na^+ currents from other currents in muscle, CsF (see below, "Solutions") was applied to the cut ends of the fiber (in pools C and E) to block K^+ and Ca^{2+} currents. Fibers were also transiently (10–15 min) exposed to external CsF to electrically uncouple the transverse tubule system. Holding the membrane potential of the fibers at -120 m*V* in between pulses eliminated the effects of long-term inactivation. The temperature of the fibers was maintained at 20–22°C.

In order to record Na^+ currents in the presence of the test solutes, control Na^+ currents were measured in the presence of standard Ringer's solution in the A pool. After recording of Na^+ currents in Ringer's solution, the A pool solution was quickly changed (solution exchange <10 s) to a premixed test solution that contained Ringer's solution and the test solute using the procedure below.

Application of Test Solutes

In both AP and voltage-clamp experiments, test solutions were not isosmotic to Ringer's solution but contained Ringer's solution and the test solute added on a volume-to-volume basis and expressed as volume percent of test solute added. Following application of the test Ringer's solution to the fiber (voltage clamp) or whole nerve (AP recording) and the subsequent recording of Na^+ currents or APs, the solution was changed back to Ringer's solution to record postcontrol Na^+ currents/APs. When AP or Na^+ current recovery was fairly complete (>75%, mean 91.5 ± 2.6) and the Na^+ currents or APs exhibited minimal or no changes in kinetics or voltage dependence, other concentrations of the solute were applied in sequence followed by recovery periods in Ringer's solution.

Solute-Induced Secretory Granule Lysis Assay for Chloride Transport

In order to detect solute-induced membrane fluidity changes, experiments were conducted to measure changes in secretory granule Cl^- transport caused by increases in membrane fluidity induced by addition of the test compounds (solutes). Rat pancreatic secretory granules were isolated by the technique of Hopfer & Gasser (1989), and the granules were suspended in control solutions of 150 mM KCl, 20 mM 4-(2-hydroxyethyl)-1-piperazineethanesulfonic acid (HEPES, pH 7.0), 1.0 mM ethyleneglycoltetraacetic acid (EGTA) and 0.1 mM $MgSO_4$ at 37°C. Test solutions were prepared by adding various volumes of solute to the suspension solution to produce a series of hypertonic test solutions.

Intact secretory granules account for >90% of the optical density at 540 nm (OD_{540}) of the secretory granule/test solution suspension. The rate of granule lysis was monitored by determining the percent change in OD_{540}. A Beckman (Fullerton, CA) DU-64 spectrophotometer, equipped with a constant temperature controller and microprocessor-controlled sampling and analysis capabilities, was used to record the change in OD_{540} at 37°C. Granules were suspended in the control solution and various test solutions generating an OD_{540} of approximately 0.3, and the rate of lysis was followed by recording changes in OD_{540} typically for a 5-min period.

In order to test for changes in chloride transport produced by the solute-induced fluidity changes, the K^+ ionophore valinomycin (10 μg/ml) was added to granules suspended in control and test solutions; valinomycin induced a K^+ influx coupled to endogenous granule Cl^- influx. Thus, the rate of solute accumulation into the granules and subsequent granule lysis depended directly on the endogenous granule Cl^- permeability. Changes in Cl^- transport produced by the presence of the solute were measured by determining the difference in valinomycin-induced lysis rates in the presence or absence of the test solute. If the solute produced changes in membrane fluidity, valinomycin-induced K influx led to an increased Cl^- channel flux and lysis rate (Gasser, Goldsmith & Hopfer, 1990). Rate changes were expressed as mean percentage changes from control rates (absence of solute). Each solute was tested at all concentrations on at least five separate granule preparations.

Solutions

Ringer's solution contained NaCl (115 mM), KCl (2 mM), $CaCl_2$ (2 mM) and HEPES (4 mM). The pH was adjusted to 7.4 using NaOH. All test solutions were prepared using a volume-per-volume dilution of the test solutes in Ringer's solution. Solute concentrations and effective concentrations for AP block were expressed as volume percents, to be consistent with Larsen et al. (1996). The solutes used were MEK, cylclohexanone, CH_2Cl_2, chloroform and TriEA. All solutes were purchased from Sigma (St. Louis, MO).

The intracellular KCl solution used in the sucrose-gap experiments contained KCl (120 mM) and HEPES (4 mM), and the pH was adjusted to 7.4 using NaOH. The sucrose (0.22 M) used to establish the sucrose gap was made osmotically equivalent to Ringer's solution. The internal solution used in voltage-clamp experiments contained CsF (115 mM), NaF (5 mM) and HEPES (4 mM), with the pH adjusted to 7.4 using NaOH.

Statistical Analysis

Mean values are reported with their associated standard error of the mean. Two-tailed *t*-tests were used at the 0.05 significance level to test for significant statistical difference between means.

Results

Whole Nerve Experiments

Protocol to obtain concentration-response relations

Figure 1a displays a typical experiment designed to obtain concentration-response relations for the solutes used in this study. Shown in sequence are the application of MEK to a sciatic nerve at two different concentrations. "R" indicates the application of Ringer's solution to the nerve; the number accompanying "R" describes whether Ringer's solution was applied for the first, second or *n*th time. The protocol used for every experiment is described below.

APs were stimulated and recorded repetitively (at either 5- or 10-min intervals) so that the progression of time during the experiment could be observed. Thus, each successive AP observed in the two panels represents one recorded 5 min after the previous one. The envelope of AP peak heights represents the kinetics of the onset or offset of the AP block. Once a steady-state effect was achieved, the solute was washed out to observe the degree of recovery; in most cases, a steady state was observed in 30 min. Similar

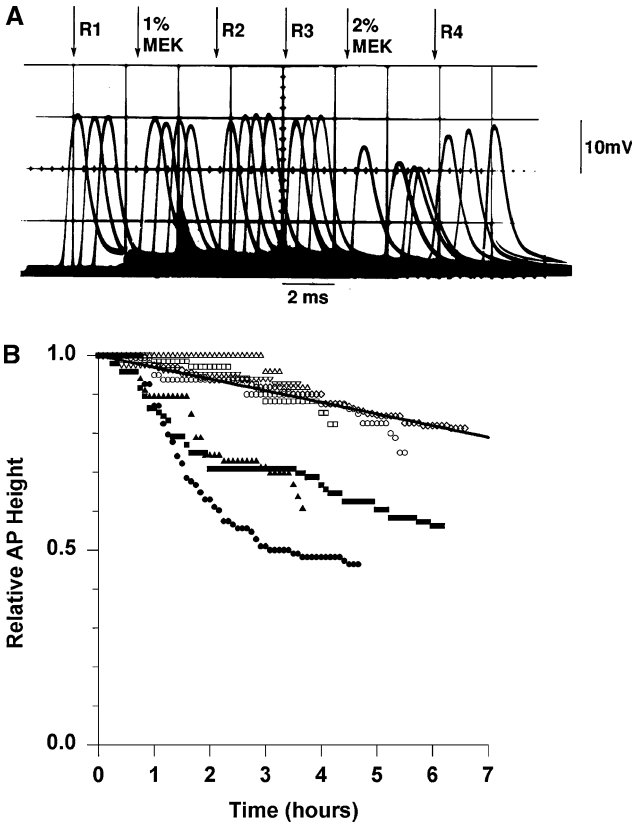

Fig. 1 MEK reversibly reduces the height of compound APs. **a** Effect of application of and removal of MEK Ringer's solution on compound APs at two different concentrations. APs were elicited and recorded every 5 min; APs were delayed and photographed every 5 min to appear in sequence on the oscilloscope and on the photograph. Shown are successive applications of MEK at 1vol% and 2vol%; MEK applications are denoted by *arrows*. Application of Ringer's solution is denoted by the symbol *R* and a number denoting the order of application. The three APs shown in Ringer's solution (denoted by *R1*) represent the first three APs recorded prior to addition of MEK Ringer's solution; 30 min of stable APs were recorded prior to MEK Ringer's solution application; however, only three are shown. **b** AP height for eight experiments designed to measure AP rundown. In these experiments, APs were recorded every 5 min and their relative heights compared to their initial height were plotted as a function of elapsed time. *Unfilled symbols* (*circles, squares, triangles, inverted triangles, diamonds*) represent five nerves that demonstrated rundown behavior that was fairly linear in time. *Solid trace* shows a linear least squares fit ($r = 0.94$) exhibiting a negative slope of 3%/h to the mean of the five nerves demonstrating fairly linear rundown. *Filled symbols* (*circles, squares, triangles*) represent three nerves showing unacceptable rundown behavior that was not fairly linear

protocols were used for all other solutes in this study, and the results were very similar (*not shown*). Four of the five solutes displaying log K_{ow}s ≥ 0.29 (MEK, $CHCL_3$, CH_2Cl_2 and cyclohexanone) showed >93% recovery even at 90–100% blocking concentrations. However, unlike the other solutes, TriEA blocked APs irreversibly, and the protocols used to study its action are described in a separate section below.

Figure 1b shows the results of control experiments designed to determine the degree of AP rundown during the course of long experiments. APs were recorded every 5 min over 4 h. APs typically showed no change in kinetics (shape) during the experiments. Experiments were accepted for analysis if rundown was <3% per hour. Experiments were corrected for rundown by assuming the AP height diminished linearly in time between control APs.

For each reversibly acting solute, one concentration was applied, followed by solute removal and recovery, before a second successive concentration was applied to the nerve. Application of low and high concentrations was randomized. Using this procedure and at least five different concentrations for each solute, concentration-response relations could be obtained for each solute. The degree of block for each concentration was defined to be the AP height in the solute divided by the preapplication control height. At least five replications of each concentration were used to obtain a concentration-response relation for each solute.

Irreversible action of TriEA

Figure 2 shows the result of applying 1.8 and 3.6 mM TriEA in Ringer's solution to a sciatic nerve previously bathed in Ringer's solution. The application of 1.8 mM TriEA was followed by two successive Ringer's solution washout periods prior to the application of TriEA at the higher concentration. The initial application of 1.8 mM TriEA caused an initial rise in the AP, followed by a continued slow decline in height until the test solution was washed out with Ringer's solution. The AP slowly declined in experiments in which TriEA was applied without Ringer's solution washouts. The first Ringer's solution washout elicited a transient increase in AP height, which then declined to a steady-state value that was not much different from the AP height in TriEA. Despite a second Ringer's solution washout, no significant recovery back to the original control AP height could be achieved. In experiments similar to the one shown in Figure 2, TriEA application typically diminished the AP height within 25 min. After 25 min, the TriEA solution was replaced by Ringer's solution. Following the Ringer's washout period, the AP recovered on average to 70% of the initial control height. Figure 2 also shows that application of 3.6 mM TriEA produced an almost complete AP block in 25 min, which recovered upon washout with Ringer's solution to 70% of its preapplication control height. Because TriEA's effect on APs was not well reversed after washout, estimates of its ability to block APs are believed to be in error by about 20% and the measurements overestimate the potency of TriEA.

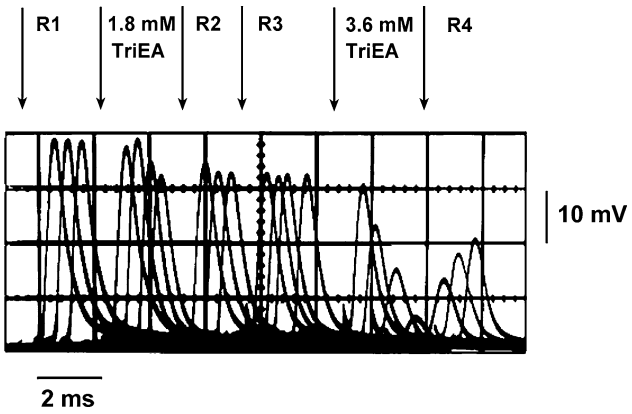

Fig. 2 TriEA irreversibly reduces the height of compound APs. The figure shows the effect of application of and removal of 1.8 and 3.6 mM TriEA Ringer's solution on compound APs. Shown are a sequence of APs elicited and recorded periodically prior to, during and following application of TriEA Ringer's solution to a whole nerve. *R1* represents the application of Ringer's solution (control) during a 15-min period; APs were recorded 5 min apart. TriEA, 1.8 mM, was applied (denoted by *arrow*), and APs were recorded immediately and 5, 15 and 25 min following the solution change. *R2* and *R3* signify two successive washouts of the chamber with Ringer's solution over a 35-min period; APs were recorded every 5 min over this period of time. Following the two successive Ringer's solution washouts, a second application of 3.6 mM TriEA Ringer's solution was applied (denoted by *arrow*) to the whole nerve. APs were recorded immediately and 5, 15 and 25 min after the solution change. Following the second TriEA application, another Ringer's solution washout application was made (denoted by *R4*). APs were recorded 5, 15 and 25 min after the solution change

In a previous report (Larsen et al., 1996), the aliphatic solute DMSO also produced an irreversible block of AP and induced shape changes in the AP. Application of large concentrations of DMSO Ringer's solution (10% DMSO Ringer's or greater) always produced changes in AP height and shape that were not reversed following Ringer's solution washouts. To obtain concentration-reponse relations for the irreversibly acting TriEA, a protocol similar to the one employed by Larsen et al. (1996) for the irreversible action of DMSO was used. The height of the AP at 25 min after TriEA application divided by the preapplication height was used to define the percent block obtained at each concentration. Although TriEA acted irreversibly to alter AP height, it did not produce the AP shape changes observed previously by Larsen et al. (1996) for the action of DMSO.

Concentration-response relations and EC_{50}s for AP block

Concentration-response relations for the five solutes are shown in Figure 3. Concentration-response curves for the solutes displaying log K_{ow}s < 0.29 were previously described in Larsen et al. (1996). In Figure 3, the solutes

are presented in order of increasing effectiveness at producing AP block (MEK < cyclohexanone < CH_2Cl_2 < $CHCL_3$ < TriEA). In each of the relations, a least squares logistic equation was used to fit the data and is shown by a solid trace; the logistic fits provide a simple method for defining an EC_{50} for each solute. When the curve fits are compared to a similar set of logistic fits for alkanols, they also provide comparative insight into the binding of aliphatic solutes to Na^+ channels. The form of the logistic equation used was as follows:

$$\%AP = \frac{A}{\left\{1 + \left(\frac{[S]}{EC_{50}}\right)^N\right\}}$$

where [S] represents the solute concentration, A is the maximum height of the AP in % and N is a slope parameter. The %AP slope is proportional to N when $[S] = EC_{50}$.

The Levenberg-Marquardt algorithm was used to obtain the best fits. The slope, N, required to obtain least squared fits to the modified logistic equation for each solute varied from a value of 2.7 to 8.0 and did not systematically change as the EC_{50}s were increased. The slope term provides insight into the binding of the molecules to the Na^+ channel protein; changes in N imply that each solute binds to a different number of binding sites. In contrast, a set of phenyl-substituted or nonsubstituted *n*-alkanols produced concentration-response relations that exhibited a slope parameter that remained constant as the length of the alkanol was increased by adding successively more methylene groups (Hahin & Kondratiev, 2001). EC_{50}s were defined to be the concentration of the logistic fit to the concentration-response relation that caused a 50% reduction in AP height from the control height. The EC_{50}s obtained from the concentration-response relations are shown in Table 1. Table 1 shows EC_{50} values (expressed in vol% and molarity) and the respective values of dV/dm, P, β and log K_{ow} for each solute. Polarity represents a measure of the high-frequency polarizability of the solute, while β provides a measure of the ability of the solute to accept a hydrogen bond with the solvent (Taft et al., 1985).

Table 1 shows that the EC_{50} values decrease as the log K_{ow} increases. Figure 4 shows that the relationship between EC_{50} and log K_{ow} can be fit with a hyperbolic function that exhibits two limiting slopes. The hyperbolic relation was obtained by obtaining a least squares linear regression of a double logarithmic plot of EC_{50} and log K_{ow}.

The more polar molecules displaying small K_{ow}s create the (left) steeply negative asymptote of the EC_{50} relation, while the molecules displaying a much greater ability to partition into octanol than water produce the (right) asymptote that approaches 0 as the log K_{ow} increases. The EC_{50} shows a correlation with P ($r = 0.7$) and β ($r = 0.56$) but surprisingly little correlation with dV/dM ($r = 0.21$). However, the EC_{50} correlates strongly with a linear combination of all three variables.

Osmotically induced attenuation of the AP

It was important to determine if block by any of the agents was produced solely by osmotic forces. Previous work conducted by Larsen et al. (1996) suggested that the solutes displaying log K_{ow}s ≤ -0.77 (DMSO, DMF and DMA) are membrane-permeant molecules and do not act to block APs by osmotic forces. DMSO, DMF and DMA are less effective at blocking APs than a simple impermeant solute. However, HMPA, the largest of the solutes used in Larsen et al. (1996) displaying a log K_{ow} of 0.28, may cause AP and Na^+ channel block by acting as a simple osmotic agent; HMPA acts similarly to sucrose in its ability to block APs and Na^+ currents. The test solutes used in the present study all are membrane-permeant and do not act as simple osmotic agents to exert their effect. In fact, the most efficacious of the five test solutes (CH_2Cl_2, $CHCl_3$ and TriEA) could not be acting as simple osmotic agents to cause AP block because they produce 50% block of APs at fairly small concentrations (<32 mM). This contrasts to the large concentration of a simple osmotic agent, sucrose (>500 mM), to produce 50% AP block.

Solute-induced changes in chloride transport

Larsen et al. (1996) showed that each of the solutes displaying log K_{ow}s < 0.29 acted to produce chloride transport–sensitive fluidity changes in pancreatic secretory vesicles at concentrations below and above EC_{50} values. Larsen et al. (1996) showed that the relative efficacy of solute-induced changes in chloride transport for the five aliphatic solutes with log K_{ow}s < 0.29 was HMPA > acetone >> DMA > DMF > DMSO. The presence of these solute-induced fluidity changes suggests that increases in membrane fluidity may play a role in AP block. A similar set of experiments was performed on the five test solutes used in this study in order to test whether they also cause membrane fluidity increases.

To test for membrane fluidity changes of all five test solutes, secretory granules were incubated in various concentrations of the solutes. Secretory vesicles behave as osmometers, and their rates of lysis are directly correlated to the rates of solute and water influx. Spectrophotometric techniques were used to estimate the relative rate of solute influx compared to H_2O efflux through the vesicle

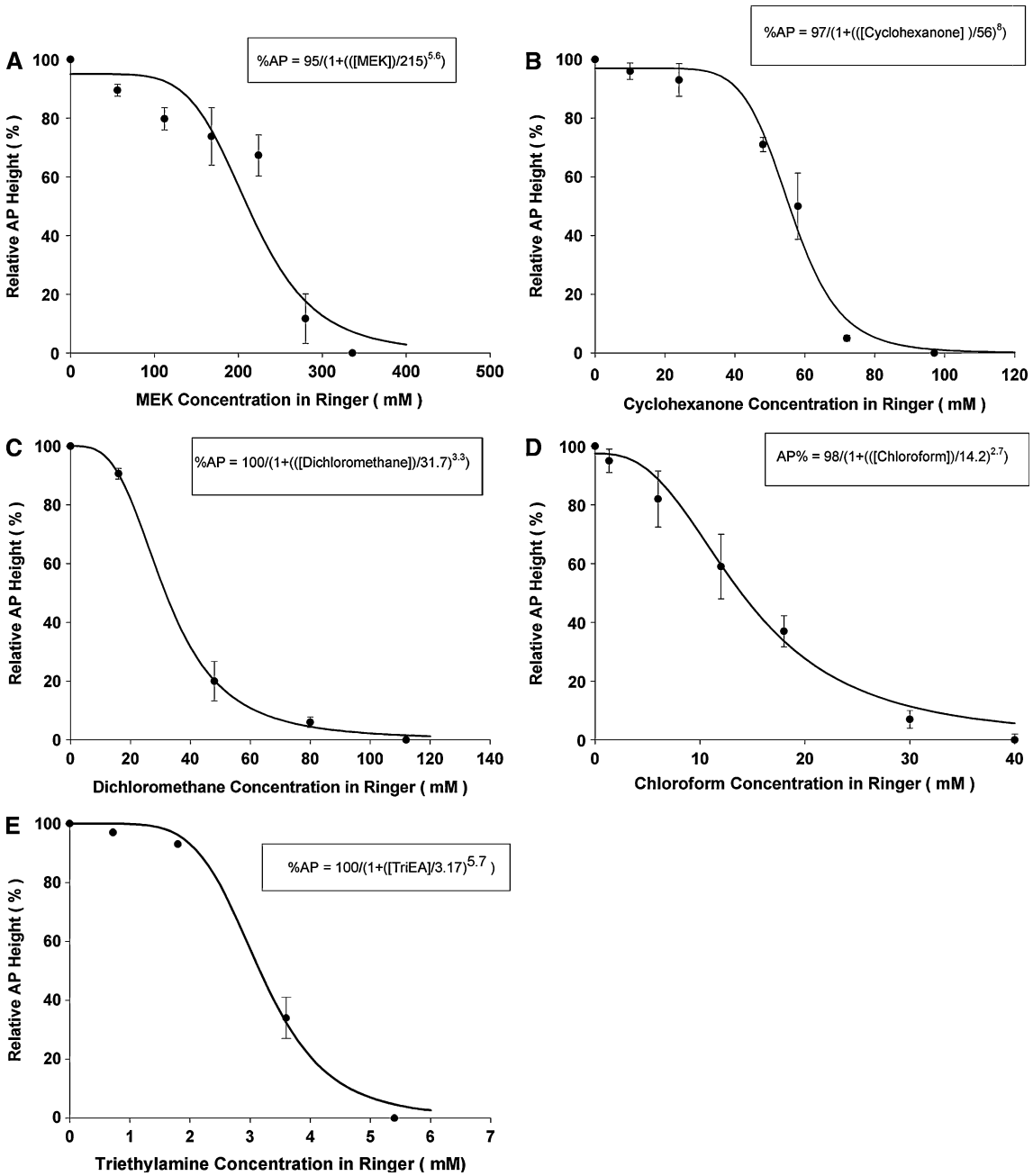

Fig. 3 Concentration-response relationships for five aliphatic solutes. **a–e** Concentration–response relationships for AP block for MEK, cyclohexanone, dichloromethane, chloroform and TriEA, respectively. Each plotted point represents the mean relative height of the AP obtained from a nerve exposed to the solute at a particular concentration, expressed as a percentage of the control height obtained in Ringer's solution. *Solid traces*, logistic fits to concentration–response relations. Error bars represent standard error

membranes. Additional experiments were conducted to determine whether the solutes acted to alter vesicle membrane fluidity reported by changes in Cl^- permeability. Previous experiments (Gasser et al., 1990) have shown that increases in secretory granule membrane fluidity produced by the addition of membrane fluidizing agents to the vesicle bathing solution that partition into the bilayer strongly correlate with increases in secretory granule Cl^- transport.

The solutes were applied to a buffered test KCl solution (for composition of the solution, see "Methods") at different concentrations to pancreatic secretory vesicles either in the absence or in the presence of the ionophore valinomycin. A change in lysis rate in the presence of valinomycin can be attributed to changes in chloride transport produced by solute-induced changes in membrane fluidity.

Table 1 ED_{50} values and physical properties of solutes

Solute	ED_{50} (% vol)	ED_{50} (mM)	dV/dm (ml/mol x 10^{-2})	P	ß	log K_{ow}
TriEA	0.045	3	1.401	0.14	0.71	1.45
Chloroform	0.12	14	0.805	0.38	0.10	1.94
Dichloromethane	0.21	32	0.624	0.62	0.10	1.15
Cyclohexanone	0.57	56	1.136	0.76	0.53	0.81
MEK	1.7	215	0.895	0.67	0.48	0.29
Acetone	4.5[a]	613[a]	0.706	0.27	0.47	0.10
HMPA	6.5[a]	373[a]	1.750	0.87	1.05	0.28
DMA	13.0[a]	1,400[a]	0.924	0.88	0.76	−0.77
DMF	12.5[a]	1,600[a]	0.774	0.88	0.69	−1.01
DMSO	20.0[a]	2,800[a]	0.710	1.00	0.76	−1.35

[a] Data obtained from Larsen et al. (1996). dV/dm, P, β and log K_{ow} values obtained from Taft et al. (1985)

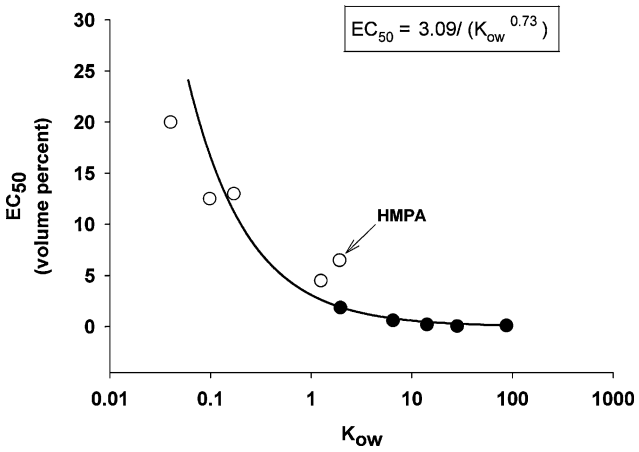

Fig. 4 EC_{50} vs. K_{ow} relation. EC_{50} estimates obtained from Figure 3a–e plotted as a function of log K_{ow}. *Open circles* represent data obtained from Larsen et al. (1996), while *filled circles* represent data obtained from Figure 3. The EC_{50} for HMPA is indicated by an *arrow*. *Solid trace*, hyperbolic decay fit to data

Cyclohexanone and CH_2Cl_2 were applied at 0.1–0.75% in increments of 0.25%, while $CHCl_3$ and TriEA were applied at 0.067%, 0.1% and 0.25% to the secretory vesicles.

Only cyclohexanone produced a significant increase in lysis rate at a concentration (0.75%) greater than its corresponding EC_{50} (0.55%, or 53 mM). At concentrations of 0.5% and below, no significant increases in lysis rate were observed. Each of the other solutes (MEK, CH_2CL_2, $CHCL_3$ and TriEA) did not significantly increase the lysis rate at any concentration tested (below or above their corresponding EC_{50} values). These results suggest that the solutes displaying log K_{ow}s of 0.29 or greater produce nominal, if any, changes in membrane fluidity at the concentrations used. The results also suggest that AP block cannot be attributed to solute-induced increases in membrane fluidity.

Muscle Voltage-Clamp Experiments

Since Na^+ channels are the principal sources of current for AP production, experiments were conducted to test whether the five solutes act to alter the size and kinetic properties of Na^+ currents. Larsen et al. (1996) showed previously that the solutes with log K_{ow}s < 0.29 act to block Na^+ currents with minimal or no effect on kinetics; therefore, it was prudent to check if the solutes with K_{ow}s ≥ 0.29 acted similarly.

Cyclohexanone, MEK, CH_2Cl_2, $CHCl_3$ and TriEA block muscle Na^+ currents

Each solute was applied externally (in Ringer's solution) to muscle, to determine its effect on Na^+ currents. Na^+ currents were elicited with test pulses to 0 m*V* (from a holding potential of -120 m*V*). Figures 5 and 6 show the results of two experiments conducted using 50 mM cyclohexanone and 30 mM CH_2Cl_2, respectively. The top of each figure shows the voltage protocol used to elicit Na^+ currents, shown below the voltage pulse. Each record shows an initial outward (upward deflection) capacitive current (elicited by the start of the depolarizing pulse), followed by an inward Na^+ current that peaks and decays. Two Na^+ current records are shown in each figure. The larger of the two represents the preapplication Na^+ current (control), while the smaller one (designated by an arrow) represents the current after solute application.

At small depolarizing voltages, muscle Na^+ currents (I_{Na}) exhibit fast and slow inactivation decays (Hahin, 1990), which were most observable at -40 m*V*. The slow decay is likely produced by the decay of activated slow Na^+ channels (Hahin, 1990), which typically contribute <6% of the total Na^+ current; to minimize the contribution of the slow component to the current kinetics, muscle fibers

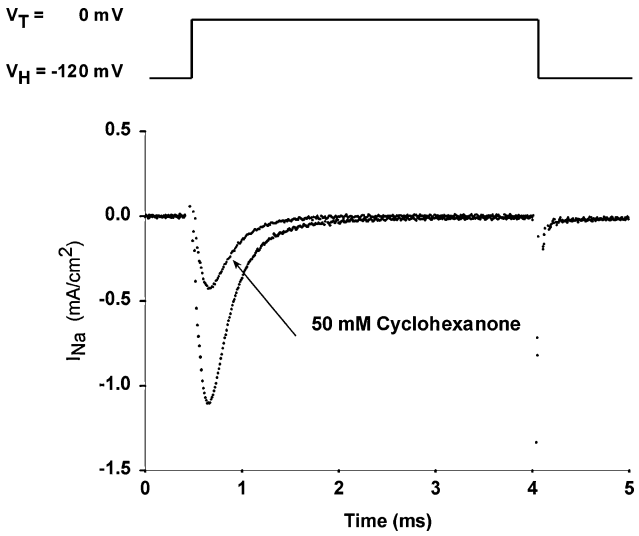

Fig. 5 Cyclohexanone attenuates Na currents with little change in kinetics. Shown are single muscle fiber Na^+ currents elicited by test pulses of 0 m*V* from a holding voltage of -120 m*V*. The pulse protocol used is shown above the current records. Currents were obtained from fibers bathed in Ringer's solution and 50 mM cyclohexanone Ringer's solution (denoted by *arrow*). T = 20°C

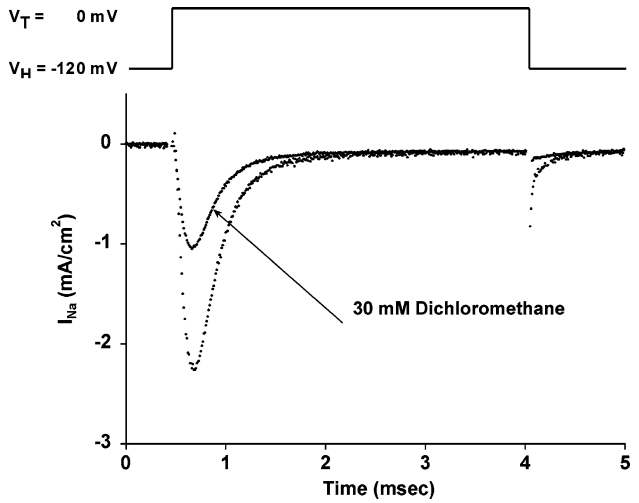

Fig. 6 Dichloromethane attenuates Na currents with little change in kinetics. Shown are single muscle fiber Na^+ currents elicited by test pulses of 0 m*V* from a holding voltage of -120 m*V*. The pulse protocol used is shown above the current records. Currents were obtained from fibers bathed in Ringer's solution and 30 mM cyclohexanone Ringer's solution (denoted by *arrow*). T = 20°C

were chosen that showed slow components that contributed 3% or less to the total Na^+ current.

Each of the five solutes was applied in Ringer's solution to single voltage-clamped muscle fibers to test their effects on the amplitude and kinetics of I_{Na}. Each of the solutes reduced Na^+ currents and blocked them completely if they were applied at concentrations much greater than the EC_{50} for AP block. To compare the kinetics of I_{Na} in the presence of each solute, solute-modified currents were scaled up (*not shown*) so that their peak values matched their corresponding pre-application control peak I_{Na}s. The two solutes shown were chosen because they typically displayed the most visible changes in kinetics. Two of the other solutes (TriEA and MEK, *not shown*) produced only small changes in the kinetic properties of I_{Na}, and chloroform produced changes that were very similar to dichlormethane. A systematic study of the kinetic alterations of I_{Na} produced by each solute was not undertaken; however, Table 2 illustrates the changes produced by the solutes. Table 2 shows estimates of the ratios of I_{Na} activation and inactivation time constants in the test solute relative to their values in Ringer's solution. Time constants were obtained using a modified Hodgkin-Huxley kinetic model (Hodgkin & Huxley, 1952) for I_{Na} to simplify the analysis. CH_2Cl_2 reduction of I_{Na} was similar to that seen for $CHCl_3$. $CHCl_3$ is an anesthetic, and its actions in reducing I_{Na} and changing channel kinetic properties have been previously reported (Haydon & Urban, 1983). CH_2Cl_2 is structurally related to $CHCl_3$ and is simply a less potent version of the anesthetic. A more systematic study of its action in altering the kinetics of I_{Na} has been previously reported (Haydon & Urban, 1983). TriEA is the most potent of the solutes used, and its action is similar to that seen for MEK, CH_2Cl_2, $CHCl_3$ or cyclohexanone. Application of the solutes at concentrations near their corresponding EC_{50} for AP block typically produced a block of 55–75% of I_{Na}; therefore, the ability of these solutes to block I_{Na} was TriEA > $CHCl_3$ > CH_2Cl_2 > cyclohexanone > MEK.

Discussion

Action and Toxicity of Aliphatic Hydrocarbons

The effects of exposure of aliphatic hydrocarbons to humans (Seppalainen, 1985) have been previously studied. Arlien-Soborg (1992) put forth hypotheses to explain how organic compounds produce neurotoxicity. He suggested

Table 2 Test solute changes in sodium current activation and inactivation

Solute	C (mM)	τ_m(S)/τ_m(R)	τ_h(S)/τ_h(R)
MEK	100	0.89 ± 0.1	0.92 ± 0.08
Cyclohexanone	50	1.05 ± 0.1	1.12 ± 0.07
Dichloromethane	30	0.78 ± 0.13	0.82 ± 0.09
Chloroform	15	0.74 ± 0.17	0.85 ± 0.1
TriEA	3	0.9	1.1

τ_m(S)/ τ_m(R), ratio of activation time constant in solute relative to Ringer's solution; τ_h(S)/τ_h(R), ratio of fast inactivation time constant in solute relative to Ringer's solution

that lipid-soluble compounds act as anesthetics to alter membrane fluidity or alter the membrane microfluidity near Na^+ channels. Our results suggest that Na^+ channel block principally contributes to aliphatic hydrocarbon AP block. Fluidity changes do not appear to be a key factor in causing block.

Biological Action of Specific Solutes

Solutes displaying small K_{ow}s (DMSO, DMF, DMA, HMPA and acetone)

The actions, properties and toxicity of DMSO, DMF, DMA, acetone and HMPA and their ability to block Na^+ channels with minimal changes in kinetic properties were previously described (Larsen et al., 1996). Each of these solutes acted to produce AP block by a combination of effects including Na^+ channel block, osmotically induced structural changes and fluidity changes (Larsen et al., 1996). As the K_{ow} of these solutes increased, Na^+ channel block played a greater role in producing AP block.

Solutes displaying larger K_{ow}s ($CHCl_3$, CH_2Cl_2, TriEA, MEK and cyclohexanone)

MEK was found to be one of the most potent solutes studied, producing neurotoxicity (Kimura et al., 1971) with an estimate of its median lethal dose (LD_{50}) of 56 mM/kg i.p. (Tanii, Tsuji & Hashimoto, 1966). Workers exposed to MEK over many years displayed abnormal nerve conduction velocities (Mitran et al., 1997). Ultrastructural studies showed that 300 μg/ml MEK for 7 weeks produced morphological abnormalities (Veronesi, 1984). Neurotoxicity by MEK is likely produced by altering ion channels associated with synaptic transmission and axonal conduction.

The oral LD_{50} of cyclohexanone in rats was reported (Smyth, Carpenter & Weil, 1969) to be 1.62 ml/kg (15 μM). Holland et al. (1990) showed that cyclohexanone acts to alter brain activity in mice and suggested that it binds to the $GABA_A$ channel. The LD_{50} reported (Smyth et al., 1969) for cyclohexanone is much smaller than the EC_{50} for AP block reported in this study. This suggests that cyclohexanone may act to bind to other ion channels with better affinity than Na^+ channels.

In neurophysiological studies (Fodor & Winneke, 1971), CH_2Cl_2 exposure (500–3,000 ppm for 3 days) to rats altered electroencephalograms and somatosensory evoked potentials. CH_2Cl_2 (5,000 ppm) produced depression of motor activity, and injections in rats slowed nerve conduction velocities. CH_2Cl_2 blocked squid axon sodium currents (Haydon & Urban, 1983) at concentrations similar to that reported in this study. Dichloromethane's alteration of Na^+ channel properties likely caused the central nervous system changes.

Haydon & Urban (1983) showed that chloroform blocked Na^+ currents in squid axons with only small changes in the current kinetics. When applied to rabbits orally in a single concentration, chloroform exhibits an LD_{50} of 2 g/kg (Torkelson, Oyen & Rowe, 1976); an LD_{50} of 2 g/kg (10 mM) is near the EC_{50} for AP block (14 mM) found in this study.

The oral LD_{50} of TriEA in rats is 0.46 g/kg (Smyth, Carpenter & Weil, 1951). A charged derivative of TriEA acts to block cardiac sarcoplasmic reticulum calcium-release channels (Tinker & Williams, 1993). In the calcium-release channel TriEA acts as an impermeant cation that blocks the pore (Tinker & Williams, 1993). It appears likely that the LD_{50} reported in rats derives from AP block.

Alkanols Block Na^+ Channels and APs Differently from Aliphatic Hydrocarbons

Alkanols are similar to local anesthetics. The potency of alkanols in producing anesthetic block correlated with the log K_{ow} (Requena & Haydon, 1985; Elliot & Haydon, 1989). AP and Na^+ channel block by phenyl-substituted primary alkanols showed that increasing their chain length increased their potency (Hahin & Kondratiev, 2001; Kondratiev & Hahin, 2001). However, unlike the concentration-response relations for aliphatic solutes which show a variety of slopes, every alkanol displayed the same slope in its concentration-response relation (Hahin & Kondratiev, 2001; Kondratiev & Hahin, 2001). This suggests that primary alkanols bind to identical locations on the Na^+ channel to exert their effect. This is consistent with a hypothesis that anesthesia is produced by binding of solutes to pockets on ion channel proteins (Heidman, Oswald & Changeux, 1983; Franks & Lieb, 1984, 1994). This study's results are consistent with the idea that aliphatic solutes bind to a number of different pockets to cause block. Since each aliphatic solute does not bind to the same pocket or set of pockets, the slope of the concentration-response curve can change.

EC_{50} Correlates with Log K_{ow}

The EC_{50}s for all 10 solutes (five in this study and five in Larsen et al., 1996) correlate ($r = -0.92$) well with their respective log K_{ow}s, showing that the molecules exhibit behavior (partition into a lipid-like substance and anesthetic action) similar to compounds studied by Overton (1901) and Meyer (1937). Overton and Meyer observed that anesthetic potency correlates with the solubility of the

molecules in olive oil, and since that time it has come to be known as the "Meyer-Overton rule." The Meyer-Overton rule or hypothesis also implied that increases in the bilayer concentration of agents alter membranes to cause anesthesia; the changes have generally been interpreted to be membrane fluidity increases because gaseous anesthetics reduce the order of lipid bilayers (Goldstein, 1984). The fluidity increases could be mimicked by small increases (ca. 1°C) in temperature. More recent work (Franks & Lieb, 1984; Larsen et al., 1996; Kondratiev & Hahin, 2001; Hahin & Kondratiev, 2001) suggests that anesthetic potency correlates with the ability of a substance to bind to membrane proteins.

To test the Meyer-Overton hypothesis, experiments were performed to measure solute-induced changes in chloride transport and I_{Na}. Solute-induced changes in chloride transport were measured to assay for ion channel–sensitive fluidity changes. Gasser et al. (1990) showed that agents added to secretory granules that increase membrane fluidity cause increased chloride transport. The results of this study show that not all solutes increase chloride transport consistently with fluidity increases. These results are inconsistent with the Meyer-Overton hypothesis. For those solutes that do produce fluidity increases, decreases in AP height (and I_{Na}) appear at concentrations well below levels that produce fluidity changes; these results suggest fluidity changes may contribute to AP block (most importantly by increasing I_{Cl}) but are not the major contributor to the block. However, these experiments do not completely rule out the Meyer-Overton hypothesis because Na^+ channels may experience a different microenvironment from chloride transporters and fluidity changes that do not alter chloride transport may alter Na^+ transport.

Voltage-clamp studies of all the solutes showed that each solute acted to reduce I_{Na} with no or minimal kinetic changes. Fluidizing agents act to speed up the kinetics of I_{Na}. Our AP and I_{Na} studies do not show any substantial speeding up in kinetic properties. Our results are best interpreted to represent a solute–ion channel interaction leading to channel block.

Experiments with the solutes displaying log K_{ow}s $<$ 0.29 (Larsen et al., 1996) were also designed to assay for osmotically induced structural changes in the whole nerve. The results of those experiments suggest that each of the solutes (with the possible exception of HMPA) does not act as a simple osmotic agent to produce AP block. However, osmotic forces do appear to cause intracellular and/or extracellular volume changes that would lead to resistance changes which contribute to reductions in AP height and shape.

The protein binding hypothesis explains most, but not all, of the results of this study. AP block appears to be produced by a combination of effects: channel block, small membrane fluidity increases and osmotically induced volume and viscosity changes. The solutes with log K_{ow}s $\geq$ 0.29 cause block at low concentrations, and thus, the first two effects predominate. The solutes with log K_{ow}s $<$ 0.29 are ineffective blockers of Na^+ channels and only block at concentrations that may cause significant osmotic effects; therefore, osmotic alterations of channel properties may contribute to AP block.

EC_{50} Follows a Hyperbolic Relation with K_{ow}

Figure 4 shows that the EC_{50} is hyperbolically related to K_{ow} using a two-parameter fit to the data. The five solutes used in this study are shown as filled circles. The open circles represent data previously obtained by Larsen et al. (1996). The slopes of the curve approach asymptotic limiting values over the region of the curve that the solutes partition well into either water (log K_{ow}s < 0) or the lipid membrane (log K_{ow}s > 1). Over the region where the solutes partition well into the bilayer, the solutes (filled circles) potently block Na^+ channels/APs and act as anesthetic/anesthetic-like molecules. Over this region, the EC_{50} relation to log K_{ow} is approximately linear. The two-parameter fit describes the behavior of four of the five solutes well. Using a double logarithmic plot of the data, Figure 7 shows that the discrepancy between the empirical relation and the data are greatest for TriEA because of TriEA's irreversible action on nerve fibers.

EC_{50} Predictions

Since EC_{50} is related to log K_{ow} and the log K_{ow} of aliphatic solutes can be well predicted as a function of dV/dm, P and β (log $K_{ow} = 0.1 + 2.9$ dV/dm $- 0.88$P $- 3.6\beta$) (Taft et al., 1985), a new equation can be constructed predicting EC_{50} as a function of dV/dm, P and β using the two-parameter model:

$$EC_{50} = 2.612\left(10^{\{-2.117[\mathrm{dv/dm}]+0.642\mathrm{P}+2.628\beta\}}\right) \quad (1)$$

The above relation is valid for aliphatic solutes only. The relation between log K_{ow} and dV/dm, P and β (Taft et al., 1985) derives from the theory of linear solvation energy relationships, which presumes that conditions exist such that general properties (e.g., solubility, chemical reactivity) of molecules (solutes) in a solvent (water) can be predicted as a linear combination of independent variables (Kamlet, Abboud & Taft, 1981). Therefore, by extension of the theory, each of the coefficients of the variables of equation 1 can also be physically interpreted. The coefficient of dV/dm represents an endoergic cavity term that represents the

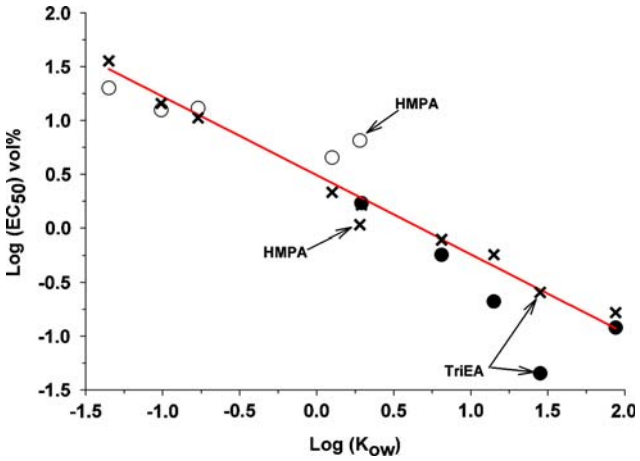

Fig. 7 EC_{50}s can be predicted as a function of P, dV/dm and ß. Shown is a double logarithmic plot of EC_{50} vs. K_{ow}. *Solid line* represents a linear best fit regression (log $[EC_{50}] = 0.49 - 0.73$[log K_{ow}], $R = -0.95$) to the data (excluding TriEA). *Crosses* represent predictions of EC_{50} obtained using equation 1. The observed and predicted values of EC_{50} for HMPA and TriEA are indicated with *arrows*

difference in energy required to produce a cavity (to contain the solute) in the bilayer compared to the solution phase. The coefficient P represents an exoergic dipolar term involving solute–solvent dipole–dipole interactions (including induced dipole interactions) that compares dipolar interactions in the bilayer and solution phase. Similarly, the coefficient β represents an exoergic hydrogen bonding term involving the solvent as donor and the solute as acceptor, which compares hydrogen binding energies in the bilayer and solution phase.

Since reductions in I_{Na} appear to be the principal cause of AP block, the simplest interpretation of the equation is that the solute can interact with Na^+ channels (via the bilayer or water phase) to produce block. The sign of the coefficient for dV/dm suggests that solute molecules principally enter the bilayer and interact with (bind to) Na^+ channels to cause reductions in I_{Na} and AP block. Similarly, solutes of high polarity that readily accept hydrogen bonds prefer to partition in the solution phase either do not block Na^+ channels or block Na^+ channels via the water phase.

Figure 7 compares the hyperbolic decay relation that best fits the EC_{50} observations shown in Figure 4 (straight line) with the calculated EC_{50}s (crosses, X) obtained from equation 1 and the actual observed EC_{50}s (circles) using a double logarithmic plot of EC_{50} and K_{ow}. Figure 7 shows that two solutes (HMPA and TriEA) are not well predicted by equation 1. TriEA acts to block APs but also to irreversibly reduce AP height by causing nerve fiber deterioration; therefore, the potency of TriEA as a channel blocker was overestimated by the data. This expectation is supported by the predicted value of the log EC_{50} for TriEA using equation 1; the predicted EC_{50} shown as a cross is higher than the observed EC_{50} (filled circle) and lies near the straight line trend established by the other solutes.

HMPA is much larger in volume than all other solutes but also is quite polarizable and an excellent hydrogen bond acceptor. In this case, equation 1 dictates that the size effect should predominate to predict a much more potent block for this solute than was observed. Thus, the three variables explain the vast majority of the variation in EC_{50} but not all the variation. Experiments conducted by Larsen et al. (1996) suggest HMPA may act as a membrane-impermeant solute that blocks Na^+ channels by osmotic forces similar to an impermeant solute such as sucrose. If HMPA acts as an impermeant solute, then equation 1 should overestimate its ability to block APs and poorly predict HMPA's observed EC_{50} as seen in Figure 7. Figure 7 illustrates the discrepancy between the observed log EC_{50} for HMPA (open circle) and the value predicted by equation 1 (X). All other predictions imply that AP block by the aliphatic solutes is predominantly produced by solute binding to Na^+ channels via the bilayer phase.

Toxicity of Solutes Correlates with EC_{50}

When mean toxicity estimates of the oral LD_{50} obtained from the Registry of Toxic Effects of Chemical Substances (*see* NIOSH, 1981) for mice and rats of the 10 solutes were plotted vs. the corresponding EC_{50} values obtained in this study and in Larsen et al. (1996), a statistically significant linear correlation ($R = 0.87$) was obtained. The mean of at least five independent estimates of the mean were used to obtain the grand means for each solute used. The relationship obtained was oral $LD_{50} = 4.49(EC_{50}) + 999$. EC_{50}s were expressed in millimoles, and LD_{50}s were expressed in milligrams per kilogram. Although AP block is not the principal cause of death as measured by the LD_{50} for most of the solutes, it plays a greater role as the solute's K_{ow} increases to cause AP block. The likelihood that death in rats and mice occurs via AP block increases as the K_{ow} increases, and this ensures that a significant correlation between EC_{50} for AP block and toxicity will exist.

AP Block Is Principally Caused by Na^+ Channel Block

The solutes act to block Na^+ channels at lower concentrations as the K_{ow} increases. The EC_{50} vs. concentration curves display different slopes, unlike the corresponding curves for alkanols; this suggests the solutes bind to Na^+ channels at more than one site. Almost all of the solutes also act on other membrane and soluble proteins, producing cytotoxicity in many other organ systems or tissues as measured by LD_{50}, toxicity and teratogenic assays. Thus,

solutes do not interact with the channels in a specific way. AP block appears to be produced by a combination of effects with the following priority:

1. Solute–channel interactions causing channel block
2. Increases in membrane fluidity causing alterations in channel properties
3. Osmotically induced cellular volume changes and channel block
4. Solute-induced changes in extracellular viscosity

As the K_{ow} increases, Na^+ channel block becomes the most significant event that causes AP block.

Acknowledgement We thank Dr. Andrei Kondratiev for performing control experiments designed to determine the rate of AP rundown. We also thank Dr. David Lotshaw for helpful discussions during the course of this work and for commenting on the manuscript. We appreciated the comments provided by an anonymous reviewer and thank the individuals for their comments.

References

Arlien-Soborg P (1992) Solvent neurotoxicity. CRC Press, Boca Raton, p 382

Elliott JR, Haydon DA (1989) The action of neutral anaesthetics on ion conductances of nerve membranes. Biochem Biophys Acta 988:257–286

Fodor GG, Winneke G (1971) Nervous system disturbances in men and animals experimentally exposed to industrial solvent vapors. In: Englund HM (ed) Proceedings of the Second International Clean Air Congress. Academic Press, New York, p 238

Franks NP, Lieb WR (1984) Do general anesthetics act by competitive binding to specific receptors? Nature 310:599–601

Franks NP, Lieb WR (1994) Molecular and cellular mechanisms of general anesthesia. Nature 367:607–614

Gasser K, Goldsmith A, Hopfer U (1990) Regulation of chloride transport in carotid secretory granules by membrane fluidity. Biochemistry 29:7282–7288

Goldstein D (1984) The effects of drugs on membrane fluidity. Annu Rev Pharmacol Toxicol 24:43–64

Hahin R (1988) Removal of inactivation causes time-invariant sodium current decays. J Gen Physiol 92:331–350

Hahin R (1990) Kinetic evidence for two Na channels in frog muscle. J Biol Physics 17:193–211

Hahin R, Campbell DT (1983) Simple shifts in the voltage dependence of sodium channel gating caused by divalent cations. J Gen Physiol 92:331–335

Hahin R, Kondratiev A (2001) ED50 AP block predictions for phenyl substituted and unsubstituted n-alkanols. J Membrane Biol 180:137–145

Hahin R, Strichartz G (1981) Effects of deuterium oxide on the rate and dissociation constants for saxitoxin and tetrodotoxin action. J Gen Physiol 78:113–139

Haydon D, Urban BW (1983) The effects of some inhalation anaesthetics on the sodium current of the squid giant axon. J Physiol 341:429–439

Heidman T, Oswald RE, Changeux J-P (1983) Multiple sites of action for noncompetitive blockers on acetylcholine receptor rich membrane fragments from *Torpedo marmorata*. Biochemistry 22:3112–3127

Hille B, Campbell DT (1976) An improved vaseline gap voltage clamp for skeletal muscle fibers. J Gen Physiol 67:265–293

Hodgkin AL, Huxley AF (1952) A quantitative description of membrane current and its applications to conduction and excitation in nerve. J Physiol 117:500–544

Holland KD, Naritoku DK, Mckeon AC, Ferrendilli JA, Covey DF (1990) Convulsant and anticonvulsant cyclopentanones and cyclohexanones. Mol Pharmacol 37:98–103

Hopfer U, Gasser K (1989) Isolation of physiologically responsive secretory granules from exocrine tissues. Methods Enzymol 174:162–172

Kamlet MJ, Abboud JLM, Taft RW (1981) An examination of linear solvation energy relationships. In: Taft RW (ed) Progress in physical organic chemistry. Wiley, New York, pp 485–630

Kimura ET, Ebert DM, Dodge PW (1971) Acute toxicity and limits of solvent residue for sixteen organic solvents. Toxicol Appl Pharmacol 19:699–704

Kondratiev A, Hahin R (2001) ED50 GNa block predictions for phenyl substituted and unsubstituted n-alkanols. J Membrane Biol 180:123–136

Larsen J, Gasser K, Hahin R (1996) An analysis of dimethylsulfoxide-induced action potential block: a comparative study of DMSO and other aliphatic water soluble solutes. Toxicol Appl Pharmacol 140:296–314

Mastrangelo CJ, Kendig JJ, Trudell JR, Cohen EN (1979) Nerve membrane lipid fluidity: opposing effects of high pressure and ethanol. Undersea Biomed Res 6:47–53

Meyer KH (1937) Contributions to the theory of narcosis. Trans Faraday Soc 33:1062–1068

Mitran E, Callender T, Orha B, Dragnea P, Botezatu G (1997) Neurotoxicity associated with occupational exposure to acetone, methyl ethyl ketone, and cyclohexanone. Environ Res 73:181–188

NIOSH (1981) Registry of Toxic Effects of Chemical Substances (RTECS). National Institute for Occupational Safety and Health, Washington DC

Overton E (1901) Studien uber die narkose. Verlag Gustaf Fischer, Jena

Requena J, Haydon DA (1985) Is there a a "cut-off" in the adsorption of long chain amphipathic molecules into lipid membranes? Biochem Biophys Acta 814:191–194

Seppalainen AM (1985) Neurophysiological aspects of the toxicity of organic solvents. Scand K Work Environ Health 11:61–64

Smyth HF Jr, Carpenter CS, Weil CS (1951) Range-finding toxicity data: list IV. Arch Ind Hyg Occup Med 4:119

Smyth HF Jr, Carpenter CS, Weil CS (1969) Range-finding toxicity data: list VII. Am Ind Hyg Assoc J 30:470–476

Strichartz GR, Sanchez V, Arthur GR, Chafetz R, Martin D (1990) Fundamental properties of local anesthetics. II. Measured octanol:buffer partition coefficients and pKa values of clinically used drugs. Anesth Analg 71:158–170

Taft RW, Abraham MH, Famni GF, Doherty RM, Abboud JM, Kamlet MJ (1985) Solubility properties in polymers and biological media 5: an analysis of the physiochemical properties which influence octanol-water partition coefficients of aliphatic and aromatic solutes. J Pharm Sci 74:807–814

Tanii H, Tsuji H, Hashimoto K (1966) Structure-toxicity relationships of monoketones. Toxicol Lett 30:13–18

Tinker A, Williams AJ (1993) Probing the structure of the conduction pathway of the sheep cardiac sarcoplasmic reticulum calcium-release channel with permeant and imperant organic cations. J Gen Physiol 102:1107–1129

Torkelson TR, Oyen F, Rowe VK (1976) The toxicity of chloroform as determined by single and repeated exposure of laboratory animals. Am Ind Hyg Assoc J 37:697–705

Veronesi B (1984) An ultrastructural study of methyl ethyl ketone's effect on cultured nerve tissues. Neurotoxicology 5:31–43